Westerfield, in *Signals and Sense: Local and Global Order in Perceptual Maps*, G. M. Edelman, W. E. Gall, W. M. Cowan, Eds. (Wiley, New York, 1990), pp. 561–588.
3. G. S. Stent, *Philos. Trans. R. Soc. London Ser. B* **312**, 3 (1985); C. B. Kimmel, in *Molecular Approaches Toward Supracellular Phenomena*, S. Roth, Ed. (Univ. of Pennsylvania Press, Philadelphia, 1990), pp. 137–174.
4. Embryos of the zebrafish, *Brachydanio rerio*, were obtained from our laboratory colony and maintained as described (*18*). The developmental stage of embryos was evaluated by the number of somite pairs; there are six pairs at 12 h and two pairs are added per hour until the embryo has 30 pairs [E. Hanneman, B. Trevarrow, W. K. Metcalfe, C. B. Kimmel, M. Westerfield, *Development* **103**, 49 (1988)]. Donor embryos were labeled at the 1- to 16-cell stage by injecting the yolk cell with 5 to 10% rhodamine-dextran as described [R. K. Ho and D. Kane, *Nature* **348**, 728 (1990)]. The label rapidly diffused into all of the blastomeres by way of cytoplasmic bridges. Embryos developed until primary motoneurons could be identified by morphological criteria (*5, 7*). One or two identified motoneurons were removed from the donor embryo by aspiration with a micropipette that was prepared on a Flaming-Brown P80/PC micropipette puller (Sutler Instrument Co.); tips were broken manually to a diameter of 8 to 12 μm. Micropipettes were backfilled with light mineral oil, and connected to a 10-μl Hamilton syringe by means of mineral oil–filled polyethylene tubing. A labeled donor embryo and an unlabeled host embryo were mounted side by side in agar (*7*). The labeled cells were expelled into the host embryo by gentle pressure. Only a single, large cell was placed in any one spinal segment. For all of the experiments described in this paper, the native primary motoneurons were eliminated from recipient spinal segments by aspiration before the transplant, although their elimination was not verified in every case. The development of transplanted cells was followed with a low-light level video system. Bright-field and fluorescence images were stored separately on optical disk. Images were processed to enhance contrast and to add multiple focal planes, bright-field, and fluorescence images on a MacIntosh computer with NeuroVideo and Image software.
5. J. S. Eisen, S. H. Pike, B. Romancier, *J. Neurosci.* **10**, 34 (1990).
6. All muscle segments are innervated by three primary motoneurons; in approximately half of the muscle segments, there is a fourth primary motoneuron that is named VaP, for its variable presence (*5*).
7. J. S. Eisen, S. H. Pike, B. Debu, *Neuron* **2**, 1097 (1989).
8. S. H. Pike and J. S. Eisen, *J. Neurosci.* **10**, 44 (1990).
9. In ten trials, one or two neurons were removed from embryos ranging in age from 16 to 18 h. In nine of these trials, each of the four motoneurons—CaP, VaP, MiP, and RoP—was positively identified, whether removed or remaining. In one trial, three cells were positively identified—including the removed MiP—and one cell, RoP, remained unaccounted for.
10. Single cells were taken from the CaP position of segments in which a VaP was not present, or a pair of cells were taken from the CaP and VaP positions of the same donor segment—at this early stage, it is not possible to distinguish CaP from VaP (*5*). Cells from both the CaP and VaP positions of a single segment can develop as normal CaPs when transplanted to a host in which the native primary motoneurons have been removed (*17*). These cells thus appear to have equivalent developmental potentials.
11. Some motoneurons were moved to the same segmental level; for example, from segment 7 to segment 7. Other motoneurons were moved to new segmental levels; for example, from segment 7 to segment 11.
12. C. Lance-Jones, *Dev. Biol.* **126**, 408 (1988); D. H. Sanes and M. Poo, *Neuron* **2**, 1237 (1989).
13. J. Y. Kuwada, R. R. Bernhardt, A. B. Chitnis, *J. Neurosci.* **10**, 1299 (1990).
14. I. S. Alverez and G. C. Schoenwolf, *Development*, in press.
15. An equivalence group comprises cells that normally develop different individual identities but which can develop the same identities under particular, abnormal conditions [J. Kimble, J. Sulston, J. White, in *Cell Lineage, Stem Cells and Determination*, N. Le Douarin, Ed. (INSERM Symposium No. 10) (Elsevier, Amsterdam, 1979), pp. 59–68].
16. K. Hatta, R. K. Ho, C. Walker, C. B. Kimmel, *Soc. Neurosci. Abstr.* **16**, 310 (1990).
17. J. S. Eisen, unpublished data.
18. J. S. Eisen, P. Z. Myers, M. Westerfield, *Nature* **320**, 269 (1986).
19. I thank E. Brandenburg, S. Poston, E. Sullivan, G. Gleason, and S. Detroy for technical assistance; C. Kimmel, M. Westerfield, and P. O'Day for comments on earlier versions of the manuscript; and P. Z. Myers for the NeuroVideo software. Supported by NIH NS23915, NIH HD22486, NSF BNS8553146, the Procter and Gamble Company, and the Murdock Charitable Trust.

6 August 1990; accepted 22 January 1991

OPC-21268, An Orally Effective, Nonpeptide Vasopressin V1 Receptor Antagonist

YOSHITAKA YAMAMURA,* HIDENORI OGAWA, TOMIHIKO CHIHARA, KAZUMI KONDO, TOSHIYUKI ONOGAWA, SHIGEKI NAKAMURA, TOYOKI MORI, MICHIAKI TOMINAGA, YOUICHI YABUUCHI

An orally effective, nonpeptide, vasopressin V1 receptor antagonist, OPC-21268, has been identified. This compound selectively antagonized binding to the V1 subtype of the vasopressin receptor in a competitive manner. In vivo, the compound acted as a specific antagonist of arginine vasopressin (AVP)–induced vasoconstriction. After oral administration in conscious rats, the compound also antagonized pressor responses to AVP. OPC-21268 can be used to study the physiological role of AVP and may be therapeutically useful in the treatment of hypertension and congestive heart failure.

TWO SUBTYPES OF PERIPHERAL AVP receptors have been distinguished both functionally and pharmacologically. In kidney, AVP exerts an antidiuretic effect through V2 vasporessin receptors by an adenosine 3′,5′-monophosphate (cAMP)–dependent mechanism (*1*). In liver and vascular smooth muscle, AVP elicits glycogenolysis and vasoconstriction, respectively, through V1 receptors by a cAMP-independent mechanism that is coupled to phosphoinositide turnover (*2*). Although many vasopressin antagonists have been developed for therapeutic use, these antagonists are all peptide analogs (*3*) and therefore do not have high enough oral bioavailability. We now describe a nonpeptide V1 vasopressin receptor antagonist, OPC-21268 (1-{1-[4-(3-acetylaminopropoxy)benzoyl]-4-piperidyl}-3,4-dihydro-2(1*H*)-quinolinone) (Fig. 1), which was developed by optimization of the lead molecule found from random screening of several thousands of compounds.

AVP and OPC-21268 both displace ^{3}H-labeled AVP bound to rat liver (V1 receptor) and kidney (V2 receptor) plasma membranes (Fig. 2). OPC-21268, at concentrations of 10^{-7} to 10^{-5} M, caused a concentration-dependent displacement of [^{3}H]AVP binding to V1 receptors, but the inhibitory effect of OPC-21268 on V2 receptor binding was weak. The concentration of OPC-21268 that displaced 50% of specific AVP binding (IC_{50}) was 4×10^{-7} M for V1 receptors and $>10^{-4}$ M for V2 receptors. From the IC_{50}, we calculated the inhibition constant (K_i) of OPC-21268 for V1 receptors (1.4×10^{-7} M). To determine if OPC-21268 interacts competitively or noncompetitively with V1 receptors, we analyzed [^{3}H]AVP binding data from rat liver membranes in the presence and absence of OPC-21268 by the Lineweaver-Burk method. OPC-21268 reduced the slope but did not change the y-axis intercept (Fig. 2B). These data indicate that OPC-21268 inhibited [^{3}H]AVP binding by changing the dissociation constant (K_d) but without changing the maximum number of receptors (B_{max}). Thus, OPC-21268 interacts competitively with V1 receptors. The K_d (1×10^{-7} M) of OPC-21268 for V1 receptors was consistent with the K_i obtained from displacement experiments. These data suggest that OPC-21268 selectively antagonized V1 receptors in vitro.

To study whether OPC-21268 acts as a specific antagonist of V1 receptors in vivo, we examined the effects of intravenous OPC-21268 administration in pithed rats

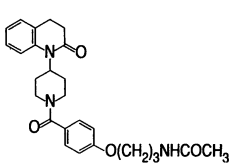

Fig. 1. Structure of OPC-21268, 1-{1-[4-(3-acetylaminopropoxy) benzoyl]-4-piperidyl}-3,4-dihydro-2(1*H*)-quinolinone.

Second Tokushima Institute of New Drug Research, Otsuka Pharmaceutical Co., 463-10 Kagasuno Kawauchi-cho Tokushima 771-01, Japan.

*To whom correspondence should be addressed.

(male Sprague-Dawley rats, 300 to 400 g, Charles River Labs). OPC-21268, at doses of 1, 3, and 10 mg per kilogram of body weight, injected intravenously (i.v.), did not alter pressor responses to angiotensin II (0.3 μg/kg i.v.) or norepinephrine (3 μg/kg i.v.), but OPC-21268 at doses of 0.03 to 1 mg/kg i.v. produced dose-dependent inhibition of pressor responses to AVP (30 mU/kg i.v.). OPC-21268 at doses of 0.1, 0.3, and 1.0 mg/kg i.v. produced rightward parallel shifts of the dose-response curves for AVP in a dose-dependent manner (Fig. 3B). These results suggest that OPC-21268 competitively and specifically antagonized pressor responses to AVP in vivo.

Next, we tested whether OPC-21268 is effective after oral administration in conscious rats (male Sprague-Dawley rats, 300 to 400 g, Charles River Labs). Exogenously administered AVP (30 mU/kg i.v.) induced

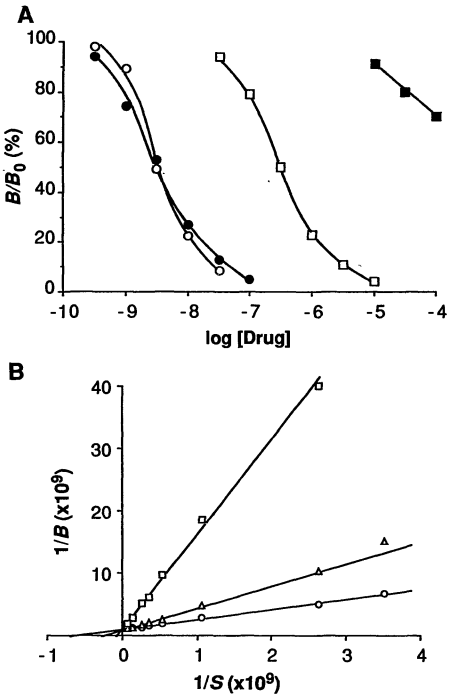

Fig. 2. In vitro antagonism of OPC-21268 to AVP. (**A**) Displacement curves of [^{3}H]AVP by AVP and OPC-21268 in rat liver plasma membranes and kidney plasma membranes. Liver and kidney plasma membranes were prepared from Sprague-Dawley rats of mass 300 to 400 g (Charles River Labs) (*4*). Protein was measured by the method of Lowry and co-workers (*5*). Various concentrations of AVP (○ and ●) and OPC-21268 (□ and ■) were incubated with 50 μg (protein equivalent) of liver membranes (open symbols) or 600 μg of kidney membranes (filled symbols) in 0.25 ml of tris buffer (100 mM, pH 8.0) containing 5 mM $MgCl_2$, 1 mM EDTA, 0.1% bovine serum albumin, and 1.9 nM [^{3}H]AVP (53.6 Ci/mmol, New England Nuclear) in the liver or 3.8 nM [^{3}H]AVP in the kidney. After incubation for 10 min at 37°C (liver membranes) or 4 hours at 4°C (kidney membranes), 3 ml of ice-cold tris buffer (100 mM, pH 8.0) was added to each assay tube, and bound and free ligands were separated by filtration through a glass microfiber filter (Whatman, GF/B) and then washed three times. Specific binding was determined by subtraction of the nonspecific binding, which was measured in the presence of 1 μM unlabeled AVP. The K_d and B_{max} of [^{3}H]AVP binding to V1 ($K_d = 4.2 \times 10^{-9}$ M, $B_{max} = 1.6 \times 10^{-12}$ mole per milligram of protein) or V2 ($K_d = 2.6 \times 10^{-9}$ M, $B_{max} = 0.66 \times 10^{-12}$ mole per milligram of protein) receptors were obtained by Scatchard analysis of saturation binding (*6*). IC_{50} values were determined from the displacement curves. (**B**) Lineweaver-Burk analysis of specific [^{3}H]AVP binding in rat liver plasma membranes in the absence (○) and presence of OPC-21268 at concentrations of 10^{-7} M (△) and 10^{-6} M (□). (*S*, [^{3}H]AVP concentration; *B* and B_0, amount of specific [^{3}H]AVP binding in the presence and absence of unlabeled compound, respectively.)

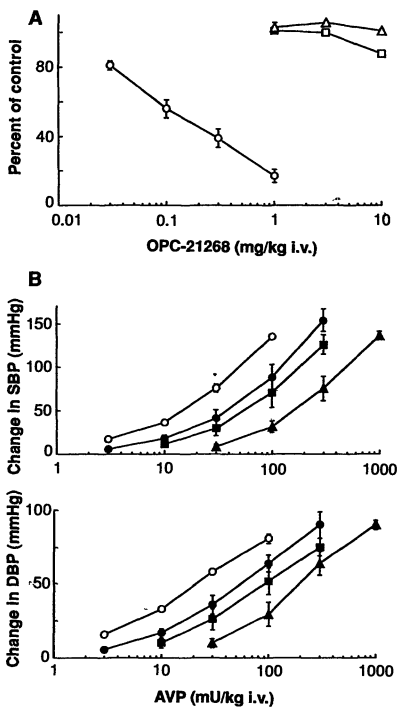

Fig. 3. In vivo antagonism and specificity of OPC-21268. (**A**) Effects of OPC-21268 on the pressor responses induced by AVP, angiotensin II, and norepinephrine in pithed rats. Their tracheae were cannulated under light ether anesthesia, and the rats were pithed as described (*7*). Immediately, artificial respiration with room air was started with a Harvard rodent respirator. The femoral artery and vein were cannulated for measurement of arterial pressure and for i.v. injection, respectively. Blood pressure was measured with a pressure transducer (MPU-0.5, NEC San-ei Instrument, Tokyo, Japan) and recorded on a thermal pen recorder (Recti-Horiz 8s, NEC San-ei Instrument). For i.v. injection, OPC-21268 was dissolved in dimethylformamide (Wako Pure Chemicals, Osaka, Japan), and other drugs were dissolved in saline. The rats were injected with drugs dissolved in a volume of 50 μl, and then with 0.2 ml of saline. OPC-21268 was given 2 min before the injection of AVP at 30 mU/kg i.v. (○), angiotensin II at 0.3 μg/kg i.v. (△), and noradrenaline at 3 μg/kg i.v. (□). Values represent mean ± SEM (n = 3). (**B**) Effects of OPC-21268 on the dose–pressor response curves for AVP in pithed rats. The dose-response curve for AVP was obtained cumulatively; each successive injection was given immediately after the maximal response of preceding dose reached. To study the effect of OPC-21268 on AVP pressor response, we injected vehicle (○) or OPC-21268, at doses of 0.1 (●), 0.3 (■), and 1.0 (▲) mg/kg i.v., 2 min before treatment with AVP. Values represent mean ± SEM (n = 4 to 8). (SBP, systolic blood pressure; DBP, diastolic blood pressure.)

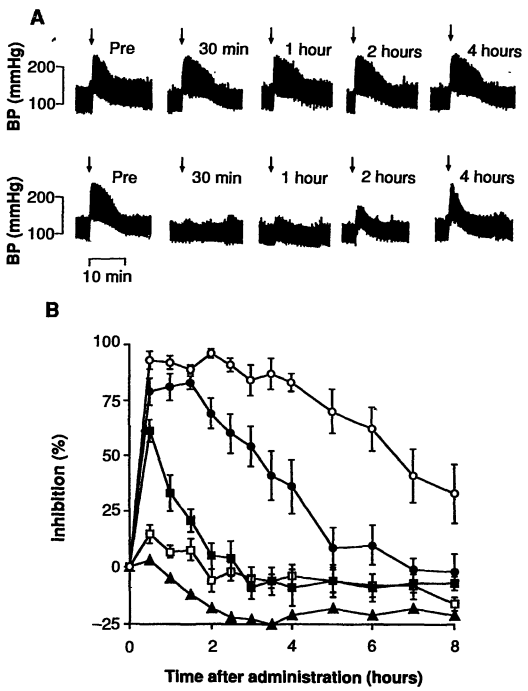

Fig. 4. Antagonism of orally administered OPC-21268 on pressor responses to AVP in conscious rats. (**A**) Typical traces are shown. (**B**) Time courses of inhibitory effects of orally administered OPC-21268. Rats were anesthetized with pentobarbitone sodium (40 mg/kg, intraperitoneally), and abdominal midsection was performed on each. A heparinized polyethylene catheter (SP-55, Natsume, Tokyo, Japan; tip with outer diameter 1.2 mm and inner diameter 0.8 mm pulled to outer diameter 0.5 mm and J-shaped by heating) was introduced into the abdominal aorta through an incision with a 26-gauge needle, and the right jugular vein was cannulated for i.v. administration. The catheters were passed subcutaneously to the dorsal side of the neck and exteriorized. After 2 to 3 days, the rats were placed in individual boxes and arterial blood pressure was measured as described in Fig. 3. After reproducible pressor responses to AVP at doses of 30 mU/kg i.v. were obtained, solvent control (5% arabic gum) (▲) and OPC-21268 at doses of 1 (□), 3 (■), 10 (●), and 30 (○) mg/kg were given orally, and pressor responses to AVP were monitored every 30 min for 8 hours after the administration. The inhibition was expressed as percent change in diastolic blood pressure (BP) increase induced by AVP before and after OPC-21268 administration. Values represent mean ± SEM (n = 4 to 5).

an increase in blood pressure in conscious rats (Fig. 4). After oral administration of OPC-21268 (10 mg/kg), the vasoconstriction induced by exogenous AVP was inhibited in a time-dependent manner (Fig. 4A). The inhibitory effect of OPC-21268 was dose-dependent, and the effect lasted for more than 8 hours at 30 mg/kg. The 50% inhibition dose (ID_{50}) for AVP-induced vasoconstriction, was estimated as 2 mg/kg. These data suggest that OPC-21268 antagonized V1 receptors after oral and i.v. administration.

We have described an orally effective, nonpeptide vasopressin V1 receptor antagonist, OPC-21268, that is more than 1000 times as selective for V1 receptors as for V2 receptors. It is expected that OPC-21268 will be a useful probe for studying the physiological or pathophysiological role of AVP.

REFERENCES AND NOTES

1. W. A. Anderson and E. Brown, *Biochim. Biophys. Acta* **67**, 674 (1963); J. Bockart, C. Roy, R. Rajerison, S. Jard, *J. Biol. Chem.* **248**, 5922 (1973).
2. M. E. M. Tolbert, A. C. White, K. Aspry, J. Cutts, J. N. Fain, *J. Biol. Chem.* **255**, 1938 (1980); M. J. Berridge and R. F. Irvine, *Nature* **212**, 315 (1984).
3. M. Manning, J. Lowbrige, C. T. Stier, J. Haldar, W. H. Sawyer, *J. Med. Chem.* **20**, 1228 (1977); M. Kruszynski, *ibid.* **23**, 364 (1980); M. Manning, B. Lammek, A. M. Kolodziejczyk, J. Seto, W. H. Sawyer, *ibid.* **24**, 701 (1981); W. H. Sawyer *et al.*, *Science* **212**, 49 (1981); M. Manning and W. H. Sawyer, *J. Lab. Clin. Med.* **114**, 617 (1989).
4. T. Nakamura, A. Tomomura, C. Noda, M. Shimoji, A. Ichihara, *J. Biol. Chem.* **258**, 9283 (1983); T. Nakahara *et al.*, *ibid.* **253**, 3211 (1978).
5. O. H. Lowry, N. J. Rosebrough, A. L. Farr, R. J. Randall, *ibid.* **193**, 265 (1951).
6. Y. Yamamura *et al.*, unpublished data.
7. J. Gillespie and T. C. Muir, *Br. J. Pharmacol. Chemother.* **30**, 78 (1967); J. T. A. Knape and P. A. van Zwieten, *Arch Int. Pharmacodyn. Ther.* **291**, 142 (1988).

8. We thank Y. Orita of Osaka University for suggestions and encouragement during this study and N. Taira of Tohoku University for review and criticism of the manuscript.

19 October 1990; accepted 1 February 1991

Uncoupling of the Spectrin-Based Skeleton from the Lipid Bilayer in Sickled Red Cells

SHIH-CHUN LIU, LAURA H. DERICK, SEN ZHAI, JIRI PALEK

The distribution of spectrin and band 3 in deoxygenated reversibly sickled cells was visualized by immunofluorescence and immunoelectron microscopy. Antibodies against band 3, the major lipid-associated transmembrane protein, labeled the entire cell body, including the entire length of the long protruding spicule, whereas antibodies against spectrin labeled only the cell body and the base region of the spicules. The results suggest that the formation of long spicules during sickling is associated with a continuous polymerization of hemoglobin S polymers, presumably through gaps in the spectrin-actin meshwork, and a subsequent uncoupling of the lipid bilayer from the submembrane skeleton.

IN ERYTHROCYTES FROM PATIENTS with sickle cell anemia, intracellular hemoglobin S (HbS) undergoes polymerization under conditions of low oxygen tension to produce sickle-shaped erythrocytes, often with long spicules protruding from the cell surface. In reversibly sickled cells (RSCs), these abnormalities disappear upon reoxygenation. In a subpopulation of erythrocytes, the irreversibly sickled cells, the abnormal shape persists after reoxygenation, despite the absence of polymerized hemoglobin in the cells (*1*). During repeated cycles of deoxygenation and reoxygenation, sickled cells shed as vesicles the part of the plasma membrane that almost completely lacks the skeletal proteins spectrin and actin (*2*). The mechanism of this membrane loss after repeated sickling is not clear. One possibility is that the lipid bilayer is uncoupled from the underlying membrane skeleton in the long protrusions. The disruption of the membrane skeleton–lipid interaction in the spicules may lead to a subsequent loss of membrane material from the sickle-shaped erythrocytes upon reoxygenation. We used the immunofluorescence and immunoelectron microscopy techniques to study the distribution of spectrin, a major skeletal protein, and band 3, a major lipid-associated, transmembrane protein, in cells undergoing deoxygenation-induced sickling in vitro.

Antibodies against band 3 labeled the whole cell body, including the entire length of the spicules. In contrast, spectrin antibodies labeled only the cell body and the base region of the spicules, but not the length of the spicules, including the tips (Fig. 1). A marked reduction in staining intensity by spectrin antibodies in the spicule regions, as compared to that in the cell body, was consistently detected, regardless of the concentrations of spectrin antibodies used. Preimmune sera or secondary antibody alone did not label the cells.

The presence of band 3, but not spectrin, in the membrane regions laminating the long spicules of the deoxygenated sickle-shaped cells was further verified by immunoelectron microscopy. Secondary antibodies conjugated with colloidal gold (15-nm diameter) were used to label spectrin and

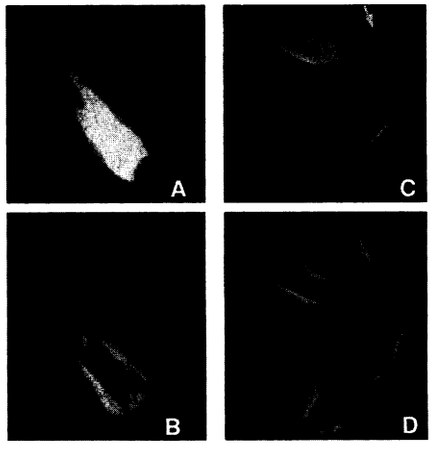

Fig. 1. Immunofluorescence labeling of band 3 (**A** and **B**) and spectrin (**C** and **D**) in deoxygenated RSCs. RSCs were isolated from patients with homozygous sickle cell disease (*11*). A 2% RSC suspension in phosphate-buffered saline (PBS) was incubated at 37°C for 1 hour under deoxygenated conditions with humidified N_2 to induce cell sickling. After incubation, cells were fixed at 25°C for 30 min with glutaraldehyde (0.1 to 0.2%, final concentration) in PBS that had been previously deoxygenated. Cells were then permeated by brief treatment (25°C, 5 min) with 0.5% Triton X-100 in PBS and washed with 0.05% Tween 20 in PBS. Affinity-purified antispectrin or antiband 3 antibodies in PBS with 1% bovine serum albumin and 0.05% Tween 20 were added to the cell sediment, and incubation proceeded with mild shaking for 1 hour at 25°C. Cells were then washed and incubated at 25°C for 1 hour with a second antibody solution of fluorescein-conjugated goat antirabbit immunoglobulin (Ig) G (Cappel, Malvern, Pennsylvania). Control samples were incubated with the secondary antibody but without the primary antibody to ensure that the secondary antibody did not cause any artificial background. The immunolabeled sickled cells were washed and examined by phase contrast (B and D) or fluorescence light (A and C) microscopy. The results show that the long spicules of deoxygenated RSCs were labeled by antibodies to band 3, but not by antibodies to spectrin (arrows).

Division of Hematology-Oncology and Departments of Biomedical Research and Medicine, St. Elizabeth's Hospital, Tufts University School of Medicine, Boston, MA 02135.